Gene 933 (2025) 148972

Contents lists available at ScienceDirect

Gene

journal homepage: www.elsevier.com/locate/gene

# Analysis of chicken *LGALSL* (galectin-related protein) gene's proximal promoter and its control by Krüppel-like factors 3 and 7

Herbert Kaltner, Gabriel García Caballero, Sebastian Schmidt *

*Department of Veterinary Sciences, Physiological Chemistry, Ludwig-Maximilians-University Munich, Lena-Christ-Str. 48, 82152 Planegg-Martinsried, Germany*

ARTICLE INFO

Edited by Nicola Lopizzo

*Keywords:*
Galectin
Galectin-related protein
Regulation
Promoter
Transcription factor
Krüppel-like factor

ABSTRACT

The *G*alectin-*R*elated *P*rotein (GRP), encoded by the *LGALSL* gene, assigned to the protein family of β-galactoside-binding Galectins, has lost carbohydrate-binding abilities. Its chicken homolog (C-GRP) occurs in the bursa of Fabricius' epithelial and B cells. Our study investigates the unknown regulatory mechanisms controlling its expression by analyzing the promoter region of the chicken *(C-)LGALSL* gene in chicken cells. We aimed to identify the sequence elements of the *C-LGALSL* gene promoter responsible for maximum activity and transcription factors (TFs) that can modulate this activity. Using luciferase reporter assays, we investigated deletion variants of the 5′ region (−2480 bp to +26 bp). Through *in silico* analyses and site-directed mutagenesis, we explored potential transcription factor binding sites, identified crucial transcription factors through transient overexpression and tested its direct binding by ChIP. Our findings highlight that the region from −274 to −75 bp, conserved among bird species, is crucial for promoter regulation. Among other tested factors, only the chicken (ch) Krüppel-like factors, chKLF3 and chKLF7, modulate the promoter's activity. The TFs chKLF3 acts as a repressor, and chKLF7 as an activator, although direct binding could not be confirmed. In conclusion, chKLF3 and chKLF7 contribute, in contrast to other factors with binding sites in the region from −274 to −75 bp, to *C-LGALSL* gene promoter regulation with a balanced impact on activity.

## 1. Introduction

Galectins (Gal) are a family of proteins characterized by the following properties: (i) they have a preferential affinity for β-galactosides, (ii) the canonical ones possess a sequence signature in their carbohydrate recognition domain (CRD) of seven amino acids, and (iii) their CRDs are arranged three-dimensionally in a β-sandwich described as a jelly-roll motif (Kaltner et al., 2019). The cellular processes in which galectins are functionally involved depend on their binding partners (ligands or counterreceptors) with which they interact. Besides extracellular glycans (on the surface of cells and microorganisms), galectins can act intracellularly sugar-independently via protein–protein interactions (Liu and Stowell, 2023). They can modulate innate and adaptive immune system cells and be involved in infection as part of the host's immune response through direct binding to microbes, wound healing, tumorigenesis, metastasis, and selective autophagy (Rodrigues et al., 2018; Ravenhill et al., 2019; Coma et al., 2023; Liu and Stowell, 2023). Galectin-related proteins are further members of the galectin family, characterized by two or more deviations in the sequence signature, resulting in loss of binding ability to the canonical β-galactosides. This subgroup includes mammalian *g*alectin-*r*elated *i*nter*f*iber prote*in* (GRIFIN), galectin-10 (Charcot-Leyden crystal protein) (Su, 2018), galectin-13 (Su et al., 2018), human GRP (hGRP) (Zhou et al., 2006; Wälti et al., 2008) and chicken GRP (C-GRP) (García Caballero et al., 2016; Manning et al., 2018), to name only a few examples. Deviations in the key residues can also lead to new sugar-binding specificities, like galectin-10 binding mannosides (Swaminathan et al., 1999).

Initially, the mRNA sequence of the hGRP (gene names *HSPC159*, *LGALSL*) was identified among 300 cDNA clones derived from human $CD34^+$ hematopoietic stem/progenitor cells (Zhang et al., 2000; Cooper, 2002). Meanwhile, one-to-one orthologues were discovered in 280 vertebrate species (Ensembl, release 112, May 2024) and detected in

*Abbreviations:* C-GRP, chicken Galectin-Related Protein; chCTCF, chicken CCCTC-binding factor; chEBF1, chicken Early B-Cell Factor 1; chEGR1, chicken Early Growth Response protein 1; CRD, carbohydrate recognition domain; EMEM, Eagles Minimum Essential Medium; Gal, Galectin; GRIFIN, galectin- related inter fiber protein; hGRP, human Galectin-related protein; IMDM, Iscove's Modified Dulbecco's Medium; KLF, Krüppel-like factors; RACE, Rapid Amplification of cDNA Ends; TFBS, transcription factor binding site; TTAG, telomere/telomerase-associated genes.

* Corresponding author.
*E-mail address:* sebastian.schmidt@lmu.de (S. Schmidt).

https://doi.org/10.1016/j.gene.2024.148972
Received 10 July 2024; Received in revised form 12 September 2024; Accepted 26 September 2024
Available online 27 September 2024

various tissues at the mRNA level, as shown for C-GRP (García Caballero et al., 2016). The amino acid sequences derived from the mRNAs show that either only two (humans and mammals) or three amino acids (e.g., birds, reptiles) of the original seven key residues in contact with the canonical ligand lactose of Gals at the CRD are conserved (Manning et al., 2018). Structurally, recombinant hGRP and C-GRP in crystallization yield the common β-sandwich fold with the two antiparallel β-sheets (Zhou et al., 2006; Wälti et al., 2008; Zhou et al., 2008; García Caballero et al., 2016).

Beyond mRNA expression, there are only a few references concerning the protein expression of GRP. The chicken orthologue, C-GRP, is present in B cells and epithelial cells of the bursa of Fabricius (Kaltner et al., 2016). In cervical adenocarcinoma cells, miR-9 mediates its tumor suppressive effect in part by downregulating protein expression of its direct target gene *HSPC159* (Zhang et al., 2016). In different breast cancer cell lines and tissue samples from breast cancer patients, upregulation of the protein expression of *HSPC159* promotes cell proliferation and worsens the prognosis of breast cancer patients (Zheng et al., 2018). These findings suggest that the hGRP protein might have an oncogenic potential. Transcriptional and post-transcriptional regulation studies may provide further indications for functional roles of GRP. Mencia et al. (2011) described regulatory effects on *HSPC159* mRNA, showing that a decreased inhibition through underexpressed miR-224, most likely in the 3′-UTR region of *HSPC159* mRNA, contributes to colon carcinoma cells' lower sensitivity to methotrexate. Only one study provides relatively sparse evidence on transcriptional regulation in the 5′-promoter region of the *HSPC159* gene (Alnafakh et al., 2020). In this study oPOSSUM analysis identified enriched potential transcription factor binding sites (TFBS) in the promoter regions of up- and down-regulated telomere/telomerase-associated genes (TTAGs) in women with endometriosis. In this context, the *HSPC159* gene is one of ten identified TTAGs, showing a down-regulated expression profile and top ten enriched TFBS (e.g., for SOX2, POU5F1, HNF1A).

Regulatory KLF proteins, 18 in mammals (13 orthologous genes in *Gallus gallus*), belong to the triple Cys2His2 zinc finger proteins and can activate or repress the expression of molecules, often in crosstalk with other co(factors). They are involved in physiological events such as endothelial functions, osteoblast differentiation, adipogenesis, cardiac regulation, or diseases such as cancer, diabetes, obesity, and osteoarthritis (García-Niño and Zazueta, 2021; Yuce and Ozkan, 2024). KLF7 has been studied in axon growth and regeneration (Wang et al., 2017; Li et al., 2018) and in several types of cancer, e.g., liver cancer (Guo et al., 2021), gastric cancer (Jiang et al., 2017), and lung cancer (Zhao et al., 2019). KLF3 is crucial in adipogenesis and obesity (Zhang et al., 2009) and colorectal cancer progression (Shen et al., 2024). Several studies have shown the transcriptional regulation of galectins by KLFs. For example, KLF15 negatively regulated *LGALS3* expression in cholesterol-loaded vascular smooth muscle cells (Li et al., 2022), KLF6 upregulated *LGALS1* (galectin-1) expression (Miranda et al., 2022), which in turn is involved in trophoblast differentiation.

Our study aims first to determine the sequence element of the *C-LGALSL* gene promoter with maximum promoter activity and second, whether chKLF3 and chKLF7 compared to other factors can change promoter activity via their specific binding sites in this sequence element.

Based on this study, our report analyzed the 5′-region of the *C-LGALSL* gene. We determined the transcription start site and the sequence region (−274/+26) responsible for luciferase reporter gene activation. The region between −274/−75 is conserved in several bird species' 5′-region of the *LGALSL* gene and contains potential binding sites for the avian transcription factors KLF3 and KLF7. In our cell models, chKLF3 repressed the promoter activity by about 50 %, while chKLF7 enhanced it by up to 300 %.

## 2. Material and methods

### 2.1. Cell culture

DT40 cells (lymphoblasts, ATCC-No. CRL-2111™) were grown in a humidified atmosphere (5 % $CO_2$) at 37 °C using Iscove's Modified Dulbecco's Medium (IMDM) supplemented with 10 % fetal calf serum, 1 % chicken serum, 1 % penicillin/streptomycin/L-glutamine solution (PSG) and 0.05 mM β-mercaptoethanol, F6CC-PR9692 (F6 cells, kindly provided by Jiri Plachý, Institute of Molecular Genetics, ASCR, Prague, Czech Republic (Plachý, 2000)) in IMDM containing 8 % fetal calf serum, 2 % chicken serum and 1 % penicillin/streptomycin/L-glutamine solution. The culture conditions of LMH cells (chicken liver hepatocellular carcinoma cell line, ATCC-No. CRL-2117™) were Eagles Minimum Essential Medium (EMEM) containing 10 % FCS and 1 % PSG solution, seeding the cells on 0.1 % gelatin-coated plastic surfaces.

### 2.2. RNA isolation and Rapid amplification of cDNA ends (RACE)

Total RNA was isolated from DT40 cells using the RNeasy Mini Kit (Qiagen, Hilden, Germany) and further processed following the Invitrogen™ GeneRacer™ Kit (Thermo Fisher Scientific, Dreieich, Germany) protocol. SuperScript™ III reverse transcriptase synthesized cDNA from RACE-ready RNA. A first round of amplification of the cDNA ends with the GeneRacer™ 5′ primer and the primer GSP1_C-GRP_rev (5′ – CTCCGACTCCCCACAGGTCAGGCTG – 3′) was followed by a nested PCR using the GeneRacer™ 5′ Nested-Primer and the primer GSP2_C-GRP_rev (5′ – GGACGATCAGCCGAGGGAAGTACACATC – 3′). The PCR fragment was isolated from agarose gel according to the instructions of the GeneRacer™ kit via S.N.A.P.™ columns and cloned into pCR™4-TOPO™ vector. The vector was commercially sequenced to determine the TSS. The determined 5′-UTR sequence of the *C-LGALSL* gene, has been deposited in the Genbank database (accession number: PQ280748).

### 2.3. Construction of C-LGALSL promoter-reporter gene vectors

Genomic DNA was extracted from F6 cells, a chicken fibroblast-like cell line, using the Wizard® Genomic DNA purification kit (Promega, Walldorf, Germany). Two DNA fragments were necessary to isolate the promoter sequence of *C-LGALSL* 2506 bp upstream of the translational start ATG. The first part (GRP-I) was amplified with the Phusion® polymerase (NEB, Frankfurt am Main, Germany) and the following primer set: forward, 5′ – CTAGGCTAGCGGCAAGAAAGGCAGGGTAATTACACC – 3′ and reverse, 5′ – TCGGTGGCGTAAACGACCTTCT – 3′. The second part of the promoter sequence (GRP-II) was isolated by using the GC-RICH PCR System (Roche, Mannheim, Germany) and the primer set: forward, 5′ – AGAAGGTCGTTTACGCCACCGA – 3′ and reverse, 5′ – GGGAAGTACACATCAGCCTGCAC – 3′. Both fragments were subcloned by TA-cloning into pGEM®-T Easy Vector (Promega). An *EcoRI* restriction site was introduced in each fragment by PCR amplification with Phusion® polymerase of both fragments using the primer sets for GRP-I (forward, 5′ – CTAGGCTAGCGGCAAGAAAGGCAGGGTAATTACACC – 3′ and reverse, 5′ – TCGGTGGCGTAAACGAATTCCTGGC – 3′) and with the GC-RICH PCR System (Roche) using the primer sets for GRP-II (forward, 5′ – GCCAGGAATTCGTTTACGCCACCGA – 3′ and reverse, 5′- GATCAAGCTTCTTGTGCGAGCGGCGGCGGC – 3′) resulting in GRP-I-EcoRI with an *EcoRI* site at the 3′ end and EcoRI-GRP-II, with an *EcoRI* site at the 5′ end. The fragments were subcloned in pGEM®-T Easy. pGEM®-T-Easy-GRP-I-EcoRI was digested with the enzymes *NheI* and *EcoRI* (all restriction enzymes were purchased from Promega), and pGEM®-T Easy-EcoRI-GRP-II with *EcoRI* and *HindIII*. The obtained fragments were then cloned into the pGL4 luciferase reporter vector (Promega) within a three-fragment ligation sample to get the vector pGL4-C-GRPp(−2480/+26). The deletion fragments were cloned accordingly. The sequences of the oligonucleotides and their respective

positions covered are shown in Supplementary Table S1. Commercial sequencing verified the correct constructs' nucleotide sequences.

### 2.4. Mutagenesis of the C-LGALSL promoter

Inserting mutations into the promoter sequence of GRPp(−274/−75) was done by QuikChange™ site-directed mutagenesis (Wang and Malcolm, 1999) with PfuTurbo DNA Polymerase (Agilent, Waldbrunn, Germany) and the primer sets listed in Supplementary Table S1.

### 2.5. Construction of transcription factor expression vectors

The coding sequences of the chicken orthologues of transcription factors (ch)CTCF, (ch)EBF1, (ch)EGR1, (ch)KLF3, (ch)KLF7, and (ch) SP1 were amplified by PCR from cDNA of DT40 cells using the primer sets listed in Supplementary Table S1. After digestion of the amplicons with the appropriate restriction enzymes, they were either subcloned (chKLF7, chSP1) into the pGEM®-T Easy (Promega) or directly cloned into the expression vector pcDNA™3.1(+) (Thermo Fisher Scientific). Constructs were commercially sequenced to verify the inserted sequences.

### 2.6. Electroporation of DT40 cells

For electroporation, $3 \times 10^6$ cells in 150 µl PBS were transferred to an ice-cold electroporation cuvette together with 50 µl PBS containing 1 µg of the pGL4-C-GRPp vectors, carrying the different promoter sequences (p), 0.5 µg pGL4.74 (*Renilla* expressing normalization vector), and 2.5 µg of an empty pGEM®-T Easy plasmid to ensure reaching the 4 µg DNA as carrier DNA. The electroporation conditions were 250 V and 950 µF for about 5 sec using the Gene Pulser® II Electroporation System (Bio-Rad, Munich, Germany). The probes were cooled on ice for 10 min and mixed with 700 µl of culture medium. Culture proceeds for 24 h in a 24-well plate mixing 300 µl of electroporated cells with 700 µl of culture medium.

### 2.7. Transfection of F6 cells

For luciferase assays, F6 cells were transfected with 500 ng of DNA using the jetPEI® transfection reagent (VWR, Darmstadt, Germany) in a ratio of 4 µl of jetPEI® per 1 µg of DNA according to the manufacturer's protocol. The cells were grown until they reached 70–80 % confluency. The transfection mixtures contain 50 ng of pGL4-C-GRPp plasmid, 10 ng pGL4.74 (*Renilla* luciferase) for normalization and, for the overexpression experiments, increasing amounts (range from 0.1 to 100 ng) of the transcription factor-expressing pcDNA3.1(+) plasmid. Each mixture was filled up with an empty pGEM®-T Easy vector to reach 500 ng DNA. After transfection, the cells were grown for about 24 h before further analysis.

### 2.8. Reportergene assays

Luciferase measurements were carried out using 20 µl of the cell lysate and following the instructions of the Dual-Luciferase® Reporter Assay System (Promega). The readout of the signals was obtained by the plate reader Infinite 200 (Tecan, Crailsheim, Germany) with an integration time of 5 sec for firefly and *Renilla* luciferase. The firefly/*Renilla* signal ratio was calculated to normalize the signal taking into account the transfection efficiency.

### 2.9. Sequence alignment (VISTA/Jalview)

For the sequence alignments, we first searched for sequences highly similar to the chicken sequence of the 500 bp 5′ upstream of the ATG of the *C-LGALSL* gene. We used the Nucleotide BLAST with a focus on highly similar sequences (megablast) and somewhat similar sequences (blastn) from the NCBI website (https://blast.ncbi.nlm.nih.gov/Blast.cgi). We then applied the 500 bp sequences of the bird species to align them using the mVISTA software (https://genome.lbl.gov/vista/mvista/submit.shtml) with a probability threshold of 0.5. This software enables the visualization of similarities and differences between DNA sequences of different species. For more detailed alignments aimed at revealing potential consensus motifs within the examined sequences, we employed Jalview (https://www.jalview.org/).

### 2.10. Computational analysis

We used the MatInspector software (Cartharius et al., 2005) from Genomatix to find potential transcription factor binding sites. For the analysis, we set the core similarity value to 1.0, which assures a perfect match to the core sequence of the binding motif, Matrix similarity was set to "optimized". The Matrix Library was version 11.1. Further, we applied the JASPAR software (https://jaspar.elixir.no) (Castro-Mondragon et al., 2022) with an 80 % threshold.

### 2.11. HaloCHIP™ procedure

The cDNAs for chicken KLF3 and KLF7 were amplified by PCR and cloned into the pHTN vector (Promega), resulting in pHTN-chKLF3 or −chKLF7. The vector encodes for the Halo-Tag, and cloning into this vector leads to a fusion protein with an N-terminal Halo-Tag (33 kDa). F6 cells were transfected within a 6-well plate using 1.5 µg of these vectors and 6 µl of jetPEI transfection reagent. After 24 h at 37 °C and 5 % $CO_2$, cross-linking was performed using IMDM containing formaldehyde at a final concentration of 1 %. After incubation for 10 min at room temperature, the reaction was quenched by adding 1.25 M glycine (pH 7.0) to a final concentration of 125 mM within medium, which caused a yellow color. After washing the cells with PBS, scraping off, centrifugation (2.000*g*, 5 min, 4 °C), and freezing the pellets at −80 °C for further processing, we followed the steps according to the manufacturer's protocol (HaloCHIP™ System, Promega).

### 2.12. RNA isolation, cDNA synthesis and quantitative PCR

The RNA was isolated using the RNeasy miniprep kit (Qiagen) following the instruction manual. For cDNA synthesis, 2 µg of total RNA was reverse transcribed applying the GoScript™ Reverse Transcriptase System (Promega) with the Oligo(dT)-Primer.

For quantitative PCR, we used 10 µl of LUNA® Universal qPCR Master Mix (NEB) in a 20 µl sample and the CFX Duet Real-Time PCR System (Bio-Rad). The data were analysed using the Bio-Rad CFX Maestro software and the Pfaffl method (Pfaffl, 2001).

### 2.13. Statistical procedures

The statistical analyses were carried out with GraphPad Prism software version 10.0.2 (GraphPad Software, Boston, MA, USA) using the non-parametric Kruskal-Wallis and Dunn's multiple comparisons test. Results were statistically significant at *$p < 0.05$, **$p < 0.01$, and ***$p < 0.001$.

## 3. Results

### 3.1. Experimental determination of the transcription start site (TSS) for the C-LGALSL gene

To analyze the promoter region, we started by determining the TSS of the *C-LGALSL* gene. RNA from chicken DT40 cells was isolated and used for a 5′-UTR RACE, as described in the material and methods section. We analyzed three clones, all revealing the same TSS, located 26 bp upstream of the translation start codon (Fig. 1). *C-LGALSL* has a TATA-less promoter since the upstream sequence does not contain a TATA box

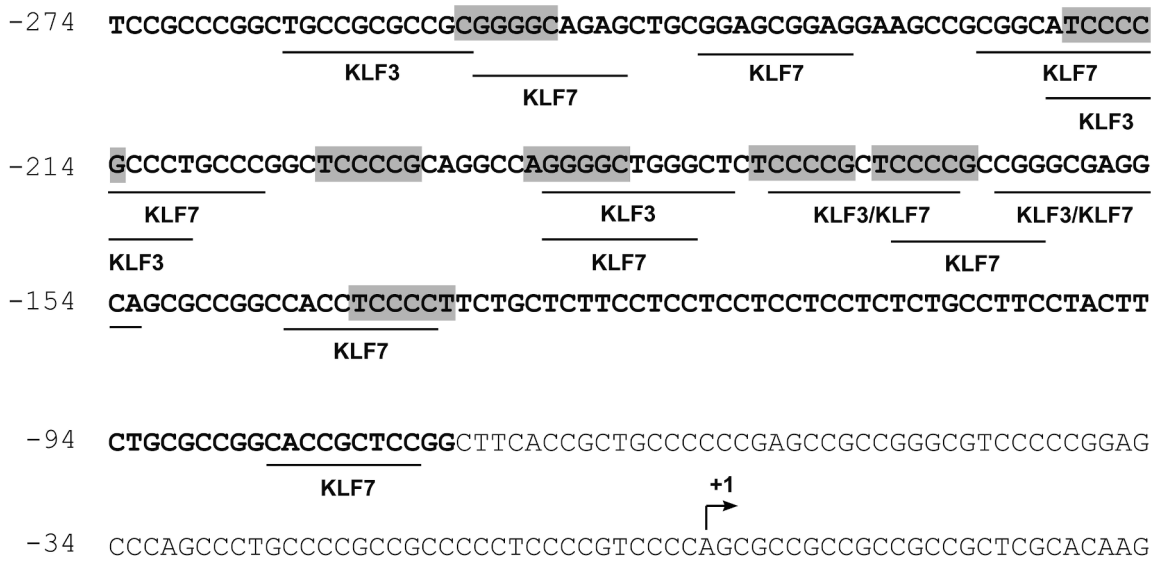


**Fig. 1.** Proximal promoter sequence of chicken *C-LGALSL* gene. The scheme shows the nucleotide sequence −274 bp/+26 bp 5′ upstream of the translational start ATG (not shown) of the *C-LGALSL* gene relative to the transcription start site (+1; black arrow). The sequence from −274 to −75 is marked in bold letters and represents the conserved region among bird species. This region is used to analyze the effects of the KLFs in reporter assays, repetitive sequence motifs are shown in grey boxes, and potential binding motifs for transcription factors KLF3 and KLF7 are underlined.

motif. The region of −500 bp relative to the TSS has a GC content of 82 %, while the sequence extension to −2500 bp still has a GC content of around 60 %.

### 3.2. Deletion analysis of the C-LGALSL promoter region

We cloned the genomic sequence upstream of the *C-LGALSL* gene, located between −2480 and +26 positions related to the determined TSS, into the promoter-less luciferase reporter vector pGL4.20 to generate the pGL4-C-GRPp(−2480/+26) reporter plasmid. The B cell lymphoma cell line DT40 (Kaltner et al., 2016) was used in initial transfection experiments to explore the promoter activity of *C-LGALSL* gene. The cloned region increased luciferase activity by 56-fold, compared to the promoter-less pGL4.20 vector (Basic, Fig. 2A). Deletion constructs made by successive shortening of the *C-LGALSL* 5′-sequence led to higher activation levels: 82-fold for pGL4-C-GRPp (−1473/+26), 153-fold for pGL4-C-GRPp(−477/+26), 153-fold for pGL4-C-GRPp(−374/+26), and 216-fold for pGL4-C-GRPp(−274/+26). Thus, we delineated a *C-LGALSL* promoter region (−274/+26) that is likely to contain the positive regulatory elements responsible for the constitutive activity. Shortening of the 5′ sequence region to pGL4-C-GRPp(−174/+26) or pGL4-C-GRPp(−74/+26) decreased the activity to 79-fold and 8.8-fold, respectively (Fig. 2A). These reduced activities indicate the loss of transcription factor binding sites in the deletion variants possibly involved in promoter activation. We also tested these promoter activities in other chicken cell lines for comparison. We transfected the fibroblast-like cell line F6 and the chicken hepatocellular carcinoma epithelial cell line LMH with the same constructs as in the DT40 cells. Similar to the DT40 cell line measurements, we observed promoter activity, with a maximum activity of up to 600-fold in the F6 cells and 50-fold in LMH cells (Supplementary Fig. S1). Also, in these cell lines, the activity decreased from −274/+26 to −174/+26 and was lowest at −74/+26.

For further characterization of the −274/+26 sequence, we generated additional variants. We started by deleting the −74/+26 sequence, as this sequence alone did show the lowest promoter activity out of all analyzed promoter sequences in our assays. We wanted to examine, how the deletion of this area affects the overall promoter activity. The resulting construct pGL4-C-GRPp(−274/−75) still reached a luciferase activity of 72-fold compared to the reference, cells transfected with the promoter-less-vector pGL4.20. For a better comparison, we again included the constructs for −274/+26 (118-fold), −174/+26 (49-fold), and −74/+26 (5-fold). The activities in this second series of measurements showed lower values compared to the promoter-less-vector (Basic) than in Fig. 2A. The relative activity to the −274/+26 sequence was 36 % (Fig. 2A) and 38 % (Fig. 2B) for −174/+26, and −74/+26 showed a relative activity of 4 % in both cases (Fig. 2A and 2B). These evaluations indicate that while the absolute values differed, the relative changes remained consistent.

When we further deleted the sequence in 20 bp increments from −274/−75 up to −174/−75, we observed a trend towards decreased luciferase activity with each deletion. Although these changes were not statistically significant, they suggest the potential importance of this sequence region (Fig. 2B). When measuring the activity of −274/−175 and comparing it to −174/−75, both fragments still show promoter activity, which indicates the importance of both sequence regions. Lastly, constructs carrying the sequences for −274/−151 and −274/−116 showed increased activity compared to −274/−175, underlining that this sequence is critical for regulatory activity. These data demonstrate that the analyzed sequence −274/−75 is highly significant in mediating gene expression. Consequently, we proceeded with further analyses focusing on this selected region.

### 3.3. LGALSL promoter region contains highly conserved sequence stretches in bird species

To address the question of whether a conserved sequence among different bird species exists, we aligned 500 bp upstream of the translation start of the *LGALSL* gene from other bird species with the respective sequence of the *C-LGALSL* gene. First, we searched for sequences related to the 5′ region of the *C-LGALSL* gene using the Basic Local Alignment Search Tool (BLAST) for nucleotide sequences (https://blast.ncbi.nlm.nih.gov/Blast.cgi).

As a result, we got 11 closely related sequences from bird species using the megablast and 103 sequences for the blastn algorithm, representing more distant bird species. We chose four sequences from each algorithm, to compare the conservation level between closely related and more distant species. This comparison included the sequences for the helmeted guineafowl (*Numida meleagris*, Gene ID: 110395439), japanese quail (*Coturnix japonica*, Gene ID: 107310673), common

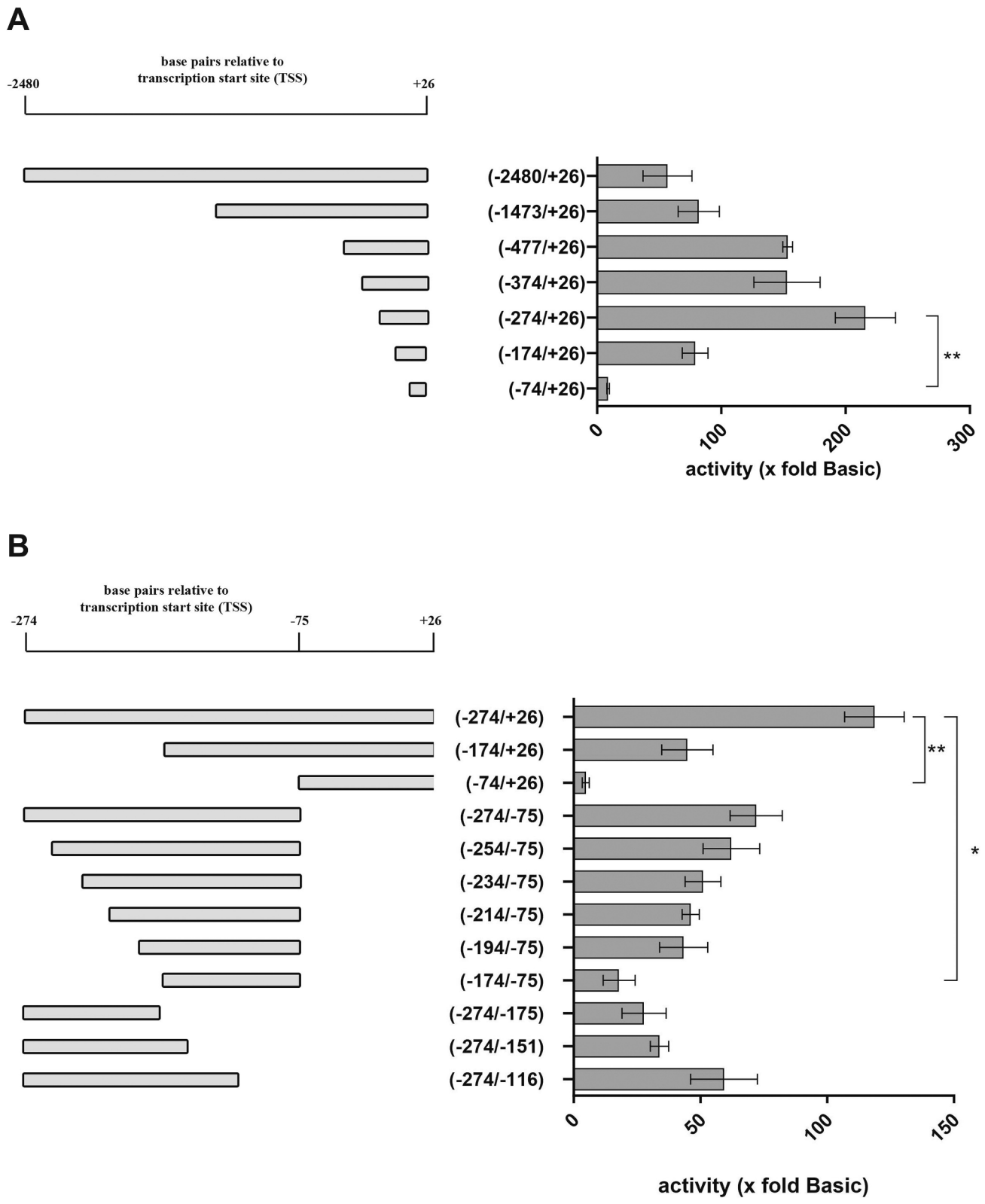


**Fig. 2.** Promoter activity of serial deletion variants of chicken *C-LGALSL* gene in DT40 cells. The promoter activity of deletion mutants shows an x-fold increase compared to cells transfected with the promoter-less vector pGL4.20 (Basic). The left bars symbolize the deletion variants drawn to scale relative to the cloned *C-LGALSL* genomic region (−2480/+26). On the right, the luciferase activities of the cloned *C-LGALSL* genomic region (−2480/+26) and the deletion variants relative to Basic are shown. A) Luciferase activities for 5′ deletions of the cloned *C-LGALSL* genomic region (−2480/+26). B) Luciferase activities for shorter 5′ and 3′ deletion variants in the area of (−274/−75) lacking −74 to +26. These variants are compared to (−274/+26), (−174/+26) and (−74/+26) deletion variants. Results show mean ± SD of three independent experiments performed in triplicates. *$p < 0.05$, **$p < 0.01$.

pheasant (*Phasanius colchicus,* Gene ID: 116232784), ruddy duck (*Oxyura jamaicensis,* Gene ID: 118163391), small tree-finch (*Camarhynchus parvulus*, Gene ID: 115902578), wire-tailed manakin (*Pipra filicauda,* Gene ID: 113982984), brown-headed cowbird (*Molothrus ater,* Gene ID: 118684852) and new caledonian crow (*Corvus moneduloides,* Gene ID: 116441524). We aligned these eight bird sequences and the human sequence as a reference for mammals and compared them to the *Gallus gallus domesticus* (chicken) sequence (Supplementary Fig. S2). We found that related birds, e.g. from the order *Galliformes*, family *Phasianidae* like helmeted guineafowl, japanese quail, and common pheasant showed a very high similarity throughout the whole sequence. The sequences of taxonomically more distant avian species, small tree-finch, wire-tailed manakin, brown-headed cowbird, and new caledonian crow, belonging to the order *Passeriformes*, and ruddy duck belonging to the order *Anseriformes*, exhibited a reduced overall similarity. An exceptional conserved region between 50 and 300 bp upstream of the start ATG, is the stretch from −24 to −274 relative to the TSS of *C-LGALSL* gene covering the sequence region responsible for the activation potential in our assays. When analyzing the sequences in more detail, we found that several sequence areas have a high grade of conservation (>80 %) throughout the species (Supplementary Fig. S2 and S3). The respective 500 bp region of the human sequence also shows conservation, but to a lesser extent (<50 %) compared to the highly conserved regions observed in bird sequences.

### 3.4. Mutational analysis of sequence motifs within the promoter region

Next, we examined the sequence region −274/−75 in more detail. We noticed a six bp sequence motif that appeared seven times within this area (Fig. 1, grey boxes). This 5′-(G/T)CCCC(G/T)-3′ motifs are at positions −254/−249 (QC1), −219/−214 (QC2), −202/−197 (QC3), −190/−185 (QC4), −177/−172 (QC5), −170/−165 (QC6) and −140/−135 (QC7) (Fig. 3A). We used site-directed mutagenesis to exchange the first and last two bp of each motif and to investigate the effect of these mutations on the promoter activity. Performing *in silico* analyses, we found that these regions refer to potential binding sites for transcription factors such as KLF3 and KLF7 (Fig. 3B). Reporter assays from lysed DT40 cells transfected with luciferase reporter vectors carrying the modified promoter fragments revealed that the activities of the variants QC2, QC4, and QC7 are lower compared to the wild-type, albeit not statistically significant (Fig. 3C). When analyzing the Jalview alignment (Supplementary Fig. S3), the areas for QC2, QC3, QC4, and QC7 are highly conserved within the analyzed bird species. We tested double and triple versions of the mutants in further experiments to investigate combinatorial effects. The double mutants, QC2/4 and QC4/7, showed further reduced activities, while QC2/7 showed an activity level comparable to that of the single mutants QC2, QC4, and QC7. The triple mutant QC2/4/7 lowered the activity by about 90 %, statistically significant, indicating a potentially involved combinatorial effect by these three sequence motifs. The results of the mutants' experiments raise the question of whether KLF3 and KLF7 or also other transcription factors could be involved in activating the *C-LGALSL* promoter.

### 3.5. chKLF3 and chKLF7 affect the activity of the −274/−75 promoter fragment of C-LGALSL

To answer this question, we analyzed in depth the *in silico* data and found that the transcription factors chCTCF, chEBF1, chEGR1, chKLF3, chKLF7, and chSP1 can all potentially bind within the −274/−75 promoter region at the 5′-(G/T)CCCC(G/T)-3′ motif. To test if these candidates can alter promoter activity, we cloned the cDNA of each candidate into the expression vector pcDNA3.1(+) and transfected F6 cells in parallel with 30 ng of these overexpression plasmids and the reporter gene vector pGL4.20 carrying the −274/−75 promoter of *C-LGALSL*. The expression of chCTCF, chEBF1, chEGR1, and chSP1 did not show any noticeable effect on the promoter activity, while chKLF3 reduced the promoter activity to 60 %. In comparison, chKLF7 expression increased it to 158 % within the cells (Fig. 4A), although not statistically significant. Different amounts of the transcription factor-expressing vectors were titrated to validate further the association between the factors and the putative regulatory element. These titration experiments allowed us to determine an apparent correlation between increasing amounts of chKLF3/chKLF7-expressing vector and luciferase activity by decreasing or increasing the promoter activity (Fig. 4B), statistically significant in both cases when using 100 ng of the TF-expressing plasmid. The areas for potential binding motifs for the KLFs are shown in the promoter sequence in Fig. 1.

### 3.6. chKLF3 and chKLF7 do not show binding to C-LGALSL promoter sequence

To analyze the binding capability to the TFBS within the promoter sequence −274/−75, we carried out a HaloCHIP™ Assay. The cDNA sequence for chKLF3 and chKLF7 were fused to the HaloTag® to generate fusion proteins. We expressed those within chicken F6 cells and cross-linked them to the genomic DNA. Following the lysis and shearing of the genomic DNA by sonication, we used the received DNA samples as a template for real-time PCR. As a positive control, we used primers on the ChIP samples to detect an area of the chicken GATA3 enhancer element interacting with chKLF7 (Sun et al., 2020). Within this control sample, we found an enrichment of the chicken GATA3 enhancer element with both transcription factors used, proving that the experimental setup is functional. We were not able to show an enrichment of the *C-LGALSL* promoter region −243/−126, the area where the TFBS for the chKLFs were suspected to be located, with either chKLF3 or chKLF7 (Supplementary Fig. S4).

## 4. Discussion

Besides the phylogenetic analysis, the critical criterion for classification as galectin-related is the three-dimensional arrangement: GRP forms the typical jelly-roll motif of galectins due to the CRD's β-sandwich fold. Compared to other members of the galectin protein family with a canonical sequence signature, C-GRP has no sugar-binding abilities due to the exchange of four of the seven amino acids forming the sequence signature to bind the primary glycan motif *N*-acetyllactosamine. Studies show that sequence segments outside the CRD are also responsible for intracellular protein interactions (Eckardt et al., 2020; Sanjurjo et al., 2022; Mayo, 2023), from which one could conclude that intracellular functional CRDs are not necessary for available interactions. On the other hand, due to the pairings of functional canonical CRDs with glycan or protein ligands (Liu and Stowell, 2023), galectins are involved in countless biological processes (Troncoso et al., 2023). A severe dilemma lies in the non-canonical CRD sequence signature of the GRP receptor: validated ligands, neither glycans nor proteins, are unknown. Thus, if the post-binding effects triggered by affine receptor-ligand pairings are unavailable, they cannot indicate functional GRP roles. How can functionality in this particular case be studied? The appearance of the *LGALSL* gene on different screens does not suggest functionality *per se*. One possible reasonable experimental approach, recognizing TFBS in the proximal promoter segment by TFs and modulating gene expression, could provide information about functional pathways in which the gene of interest is involved (Xu et al., 2022). Accordingly, we investigated by deletion constructs the 5′- promoter region 2500 bp upstream the start ATG (including the sequence downstream the TSS) of the *C-LGALSL* gene to identify relevant TFBS and validate the corresponding TFs' binding. The construct carrying the −274/+26 region of the *C-LGALSL* gene had the highest luciferase activity. When analyzing sequence stretches beyond this region, lower activities indicate repressing motifs, especially between the positions −275 to −374 and −478 to −1473. The importance of the −274/+26 proximal promoter region can be seen from the fact that the activity

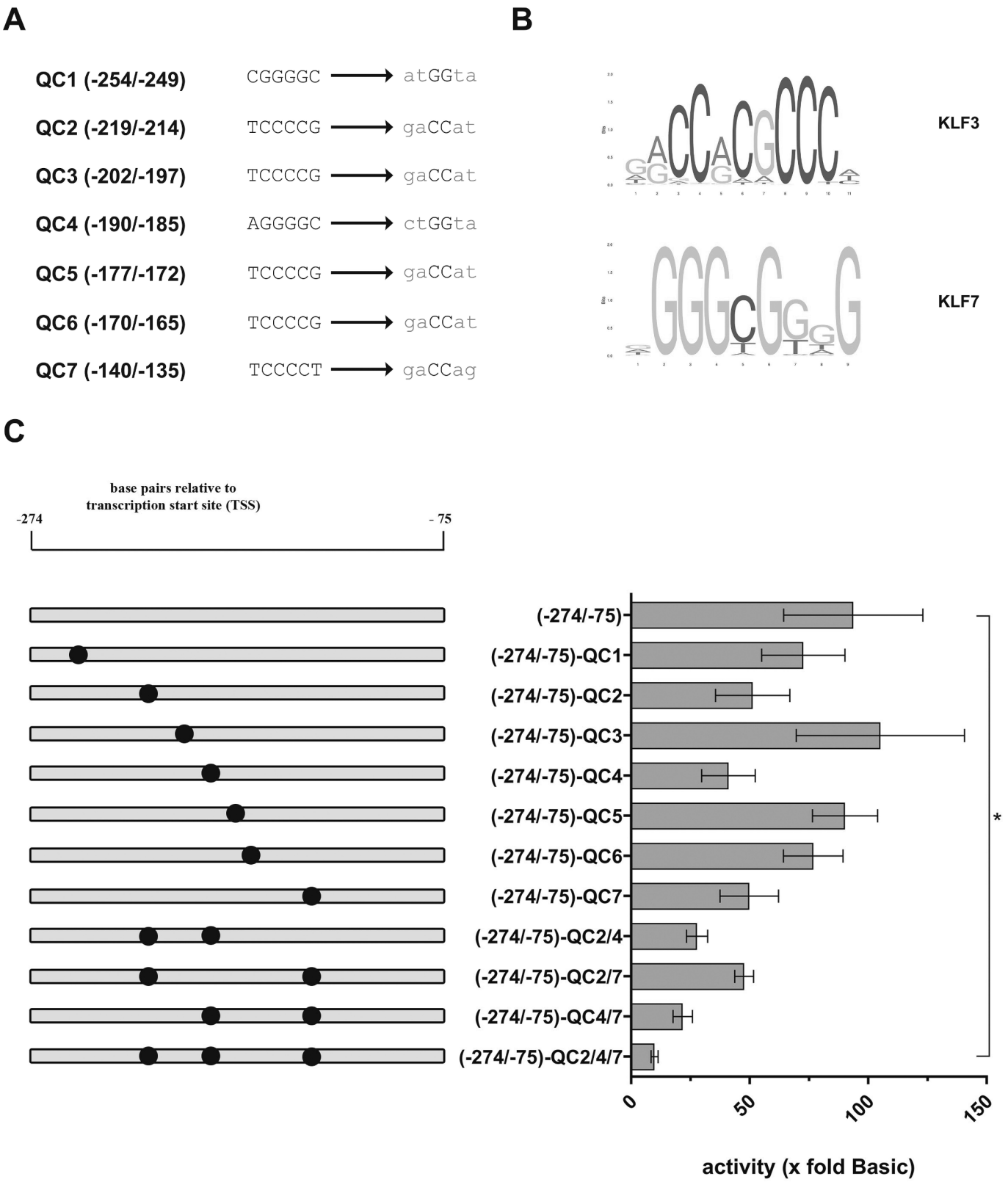


**Fig. 3.** Analysis of sequence mutants within the (−274/−75) promoter region of *C-LGALSL* gene in DT40 cells. A set of repetitive sequence motifs was detected and mutated to analyze its effect on promoter activity. A) The seven QuikChange™ (QC) positions containing the 5′-(G/T)CCCC(G/T)-3′ motifs are shown with their explicit position within the promoter region in brackets. Mutated bases are shown in small letters. B) Consensus motifs for transcription factors KLF3 (Matrix ID: MA1516.1) and KLF7 (Matrix ID: MA1959.1) from the JASPAR website. C) Luciferase activity of single and combined promoter QC mutants. The black-filled circles indicate the relative position of the respective mutation in the bars symbolizing the (−274/−75) on the left. On the right, the promoter activity is shown as x-fold activity compared to cells transfected with the pGL4.20 (Basic) vector. Results show mean ± SD of three independent experiments performed in triplicates. *$p < 0.05$.

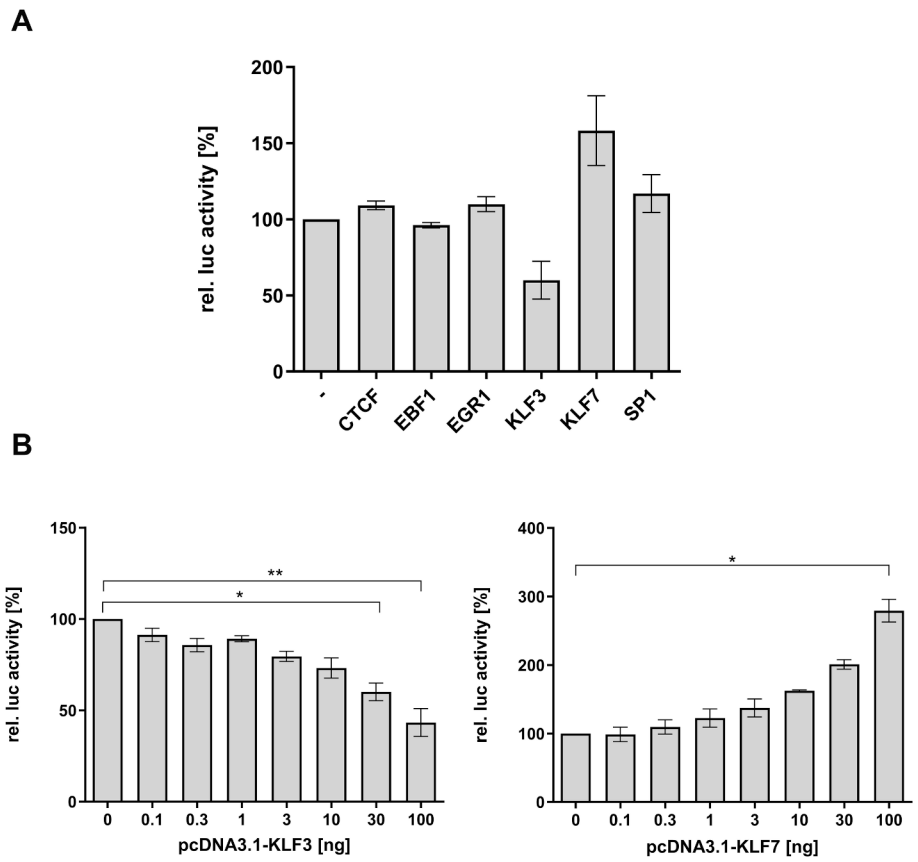


**Fig. 4.** Impact of transcription factors on the activity of the (−274/−75) promoter region of *C-LGALSL* gene. A) Luciferase activities in F6 cells transfected with 30 ng pcDNA3.1(+) plasmids containing the respective coding sequences for chicken CTCF, EBF1, EGR1, KLF3, KLF7 or SP1. Relative activity is shown as the percentage compared to mock transfection (empty pcDNA3.1). B) Luciferase activities after administration of increasing amounts of pcDNA3.1(+)-KLF3 (left) or pcDNA3.1 (+)-KLF7 vector (right). The promoter activity of GRP(−274/−75) is measured by luciferase assay as a percentage, whereas the promoter shows 100 % activity without any additional transcription factor. Results show mean ± SD of three independent experiments performed in triplicates. *p < 0.05, **p < 0.01.

decreases with every shortening of the sequence. Alignments with orthologous sequences from genomes of different bird species showed that part of this region is well-conserved (−24 to −274). It is worth mentioning that analyzing the *Gallus gallus* reference sequence (NC_052534.1), there is an additional 9 bp after the TSS resulting from a shot-gun sequencing. In detail, it is 8 'CGC' triplets, whereas our sequence or the sequences from *Numida*, *Coturnix,* and *Phasianus* contain 5 triplets (Supplementary Fig. S5). It could be due to individual variability of sequence stretches. We focused on examining a narrowed area, and *in silico* analysis indicates transcription factors that have the potential to bind the region of −274/−75. We decided to focus on that 200 bp area, as the −174/−75 and the −274/−175 regions alone have activation potential on their own, whereas −74/+26 did not. However, for maximum activity, −74/+26 also plays an important role, as −274/+26 still has higher activity than the −274/−75 region, an issue that needs to be considered in future studies. For this study, we examined the −274/−75 region and selected a set of transcription factors that can bind to a repetitive motif in this region, which is 5′-(G/T)CCCC(G/T)- 3′ and investigated their potential to activate the reporter gene expression. As a result, chKLF3 represses, and chKLF7 enhances promoter activity and potentially takes part in the regulating of *C-LGALSL*, whereas other selected and tested factors do not influence the activity.

As outlined in recent reviews, Krüppel-like factors possess three conserved zinc finger DNA binding domains and play essential roles in various physiological processes and diseases (Pollak et al., 2018; Yuce and Ozkan, 2024). KLF3 is a known transcriptional repressor that interacts with C-terminal Binding Protein 1 and 2 (CtBP1, CtBP2) as a co-repressor (Turner and Crossley, 1998). It is involved in processes of B cell development (Vu et al., 2011) and plays an essential role in erythropoiesis (Funnell et al., 2012). Furthermore, KLF3 is known to directly target the promoter of the *LGALS3* gene to repress the expression of hGal-3 (Knights et al., 2016). In this case, KLF3 is counterplayed by the EKLF/KLF1 transcription factor, which might balance the positive/negative regulation of hGal-3 expression (Funnell et al., 2012). This finding results from the similar DNA-binding preferences by KLF, which mainly involve CACCC boxes. We proved that chKLF3 and chKLF7 can also regulate the promoter of *C-LGALS3* gene (chicken galectin-3, CG-3). As with the *C-LGALSL* gene promoter, chKLF3 represses the promoter activity, and chKLF7 activates the promoter of the *C-LGALS3* gene (Supplementary Fig. S6). This observation suggests these transcription factors may be part of a shared regulatory network. KLF7 is widely expressed in the central nervous system (Laub et al., 2005; Bhattarai et al., 2016) and can support axon regeneration (Veldman et al., 2007; Blackmore et al., 2012) and also has an impact on osteoporosis (Chen et al., 2022). KLF7 interacts with KLF4 for axon growth, with KLF7 promoting growth and KLF4 suppressing it (Moore et al., 2009). These two examples from the literature show that KLF factors can act together to fine-tune gene regulation. Interestingly, in our experimental approach, we observed that repression and activation of the *C-LGALSL* promoter approximately balanced each other after simultaneous transfection of pcDNA3.1(+)-chKLF7/-chKLF3 plasmids for overexpression (data not shown). In this study, we could not verify whether chKLF3 and chKLF7 can bind to the promoter region of *C-LGALSL*, so we cannot determine whether these factors might bind to the same motif within the sequence. We can exclude a technical issue as the positive control was working, showing chKLF7 binds to the enhancer element of GATA3 (Sun

et al., 2020). Possibly, the potential binding motifs for chKLF3/chKLF7 are blocked *in vivo* by DNA methylation or histone hypo-acetylation/methylation events in F6 cells and are inaccessible to the chKLFs. One cannot rule out CtBP acting as a co-repressor in the case of chKLF3. Knights et al. (2016) reported a 2.5-fold repression of hGal-3 promoter activity under a KLF3 mutant without CtBP association. In contrast, KLF3 wild type (with CtBP interaction) showed a 4-fold repression. This finding means that the repression of promoter activity depends partially on the co-repressor CtBP in the case of human *LGALS3*. On the contrary, KLF12 binds directly to the human *LGALS1* (galectin-1) promoter, resulting in downregulated expression of hGal-1 and promoting $CD8^+$ T cell infiltration, contributing to an immune active tumor microenvironment. The findings of this study showed that promoter regulation of the galectin-1's gene (*LGALSL1*) by KLF12 strongly impacts the galectin-1 protein's involvement in specific functional pathways (Zheng et al., 2023).

In summary, we determined the *C-LGALSL* gene's proximal promoter region and enclosed the critical sequence area to −274/−75 related to the TSS. Further, we could show that chKLF3 and chKLF7 both influence the activity of the promoter in a dose-dependent manner. This study is the first to investigate the gene (*LGALSL*) regulation of a galectin-related protein, which occurs in the genome of 280 vertebrate species (Ensembl, release 112, May 2024). The TFs chKLF3 and chKLF7 are candidates involved in transcriptional regulation of *C-LGALSL*, although their mode influencing C-GRP's gene expression needs to be clarified.

## Ethical approval

Ethical review and approval were waived for this study as we used cell lines.

## Declaration of Generative AI and AI-assisted technologies in the writing process

During the preparation of this manuscript, the authors did not use any AI.

## CRediT authorship contribution statement

**Herbert Kaltner:** Writing – review & editing, Supervision. **Gabriel García Caballero:** Writing – review & editing, Investigation. **Sebastian Schmidt:** Writing – review & editing, Writing – original draft, Project administration, Investigation, Data curation, Conceptualization.

## Declaration of competing interest

The authors declare that they have no known competing financial interests or personal relationships that could have appeared to influence the work reported in this paper.

## Data availability

Data will be made available on request.

## Acknowledgements

We gratefully acknowledge the technical assistance by Christian Overdiek and Martin Vogel. We thank Dr. Joachim Manning and Dr. Sabine André for critical reading and language editing.

## Appendix A. Supplementary material

Supplementary data to this article can be found online at https://doi.org/10.1016/j.gene.2024.148972.

## References

Alnafakh, R., Choi, F., Bradfield, A., Adishesh, M., Saretzki, G., Hapangama, D.K., 2020. Endometriosis is associated with a significant increase in hTERC and altered telomere/telomerase associated genes in the eutopic endometrium, an *ex-vivo* and *in silico* study. Biomedicines 8, 588. https://doi.org/10.3390/biomedicines8120588.

Bhattarai, S., Sochacka-Marlowe, A., Crutchfield, G., Khan, R., Londraville, R., Liu, Q., 2016. Krupple-like factors 7 and 6a mRNA expression in adult zebrafish central nervous system. Gene Expr Patterns 21, 41-53. doi: 10.1016/j.gep.2016.06.004.

Blackmore, M.G., Wang, Z., Lerch, J.K., Motti, D., Zhang, Y.P., Shields, C.B., Lee, J.K., Goldberg, J.L., Lemmon, V.P., Bixby, J.L., 2012. Krüppel-like Factor 7 engineered for transcriptional activation promotes axon regeneration in the adult corticospinal tract. PNAS 109, 7517–7522. https://doi.org/10.1073/pnas.1120684109.

Cartharius, K., Frech, K., Grote, K., Klocke, B., Haltmeier, M., Klingenhoff, A., Frisch, M., Bayerlein, M. and Werner, T., 2005. MatInspector and beyond: promoter analysis based on transcription factor binding sites. Bioinformatics 21, 2933-42. doi: 10.1093/bioinformatics/bti473.

Castro-Mondragon, J.A., Riudavets-Puig, R., Rauluseviciute, I., Lemma, R.B., Turchi, L., Blanc-Mathieu, R., Lucas, J., Boddie, P., Khan, A., Manosalva Perez, N., Fornes, O., Leung, T.Y., Aguirre, A., Hammal, F., Schmelter, D., Baranasic, D., Ballester, B., Sandelin, A., Lenhard, B., Vandepoele, K., Wasserman, W.W., Parcy, F., Mathelier, A., 2022. JASPAR 2022: the 9th release of the open-access database of transcription factor binding profiles. Nucl. Acids Res. 50, D165–D173. https://doi.org/10.1093/nar/gkab1113.

Chen, C., Hu, F., Miao, S., Sun, L., Jiao, Y., Xu, M., Huang, X., Yang, Y., Zhou, R., 2022. Transcription factor KLF7 promotes osteoclast differentiation by suppressing HO-1. Front. Genet. 13, 798433. https://doi.org/10.3389/fgene.2022.798433.

Coma, M., Manning, J.C., Kaltner, H., Gal, P., 2023. The sweet side of wound healing: galectins as promising therapeutic targets in hemostasis, inflammation, proliferation, and maturation/remodeling. Expert Opin. Ther. Targets 27, 41–53. https://doi.org/10.1080/14728222.2023.2175318.

Cooper, D.N., 2002. Galectinomics: finding themes in complexity. BBA 1572, 209–231. https://doi.org/10.1016/s0304-4165(02)00310-0.

Eckardt, V., Miller, M.C., Blanchet, X., Duan, R., Leberzammer, J., Duchene, J., Soehnlein, O., Megens, R.T., Ludwig, A.K., Dregni, A., Faussner, A., Wichapong, K., Ippel, H., Dijkgraaf, I., Kaltner, H., Doring, Y., Bidzhekov, K., Hackeng, T.M., Weber, C., Gabius, H.-J., von Hundelshausen, P., Mayo, K.H., 2020. Chemokines and galectins form heterodimers to modulate inflammation. EMBO Rep. 21, e47852.

Funnell, A.P., Norton, L.J., Mak, K.S., Burdach, J., Artuz, C.M., Twine, N.A., Wilkins, M. R., Power, C.A., Hung, T.T., Perdomo, J., Koh, P., Bell-Anderson, K.S., Orkin, S.H., Fraser, S.T., Perkins, A.C., Pearson, R.C., Crossley, M., 2012. The CACCC-binding protein KLF3/BKLF represses a subset of KLF1/EKLF target genes and is required for proper erythroid maturation in vivo. Mol. Cell Biol. 32, 3281–3292. https://doi.org/10.1128/MCB.00173-12.

García Caballero, G., Flores-Ibarra, A., Michalak, M., Khasbiullina, N., Bovin, N.V., André, S., Manning, J.C., Vértesy, S., Ruiz, F.M., Kaltner, H., Kopitz, J., Romero, A., Gabius, H.-J., 2016. Galectin-related protein: An integral member of the network of chicken galectins 1. From strong sequence conservation of the gene confined to vertebrates to biochemical characteristics of the chicken protein and its crystal structure. BBA 1860, 2285–2297. https://doi.org/10.1016/j.bbagen.2016.06.001.

García-Niño, W.R., Zazueta, C., 2021. New insights of Krüppel-like transcription factors in adipogenesis and the role of their regulatory neighbors. Life Sci. 265, 118763. https://doi.org/10.1016/j.lfs.2020.118763.

Guo, Y., Chai, B., Jia, J., Yang, M., Li, Y., Zhang, R., Wang, S., Xu, J., 2021. KLF7/VPS35 axis contributes to hepatocellular carcinoma progression through CCDC85C-activated beta-catenin pathway. Cell Biosci. 11, 73. https://doi.org/10.1186/s13578-021-00585-6.

Jiang, Z., Yu, T., Fan, Z., Yang, H., Lin, X., 2017. Krüppel-Like Factor 7 is a marker of aggressive gastric cancer and poor prognosis. Cell. Physiol. Biochem. 43, 1090–1109. https://doi.org/10.1159/000481748.

Kaltner, H., García Caballero, G., Sinowatz, F., Schmidt, S., Manning, J.C., André, S., Gabius, H.-J., 2016. Galectin-related protein: An integral member of the network of chicken galectins: 2. From expression profiling to its immunocyto- and histochemical localization and application as tool for ligand detection. BBA 1860, 2298–2312. https://doi.org/10.1016/j.bbagen.2016.06.002.

Kaltner, H., Abad-Rodríguez, J., Corfield, A.P., Kopitz, J., Gabius, H.-J., 2019. The sugar code: letters and vocabulary, writers, editors and readers and biosignificance of functional glycan-lectin pairing. Biochem. J 476, 2623–2655. https://doi.org/10.1042/BCJ20170853.

Knights, A.J., Yik, J.J., Mat Jusoh, H., Norton, L.J., Funnell, A.P., Pearson, R.C., Bell-Anderson, K.S., Crossley, M., Quinlan, K.G., 2016. Krüppel-like Factor 3 (KLF3/BKLF) is required for widespread repression of the inflammatory modulator galectin-3 (Lgals3). J. Biol. Chem. 291, 16048–16058. https://doi.org/10.1074/jbc.M116.715748.

Laub, F., Lei, L., Sumiyoshi, H., Kajimura, D., Dragomir, C., Smaldone, S., Puche, A.C., Petros, T.J., Mason, C., Parada, L.F., Ramirez, F., 2005. Transcription factor KLF7 is important for neuronal morphogenesis in selected regions of the nervous system. Mol. Cell Biol. 25, 5699–5711. https://doi.org/10.1128/MCB.25.13.5699-5711.2005.

Li, J., Shen, H., Owens, G.K., Guo, L.W., 2022. SREBP1 regulates Lgals3 activation in response to cholesterol loading. Mol. Ther. Nucleic Acids 28, 892–909. https://doi.org/10.1016/j.omtn.2022.05.028.

Li, W.Y., Zhang, W.T., Cheng, Y.X., Liu, Y.C., Zhai, F.G., Sun, P., Li, H.T., Deng, L.X., Zhu, X.F., Wang, Y., 2018. Inhibition of KLF7-targeting microRNA 146b promotes sciatic nerve regeneration. Neurosci. Bull. 34, 419–437. https://doi.org/10.1007/s12264-018-0206-x.

Liu, F.T., Stowell, S.R., 2023. The role of galectins in immunity and infection. Nat. Rev. Immunol. 23, 479–494. https://doi.org/10.1038/s41577-022-00829-7.
Manning, J.C., García Caballero, G., Ruíz, F.M., Romero, A., Kaltner, H., Gabius, H.-J., 2018. Members of the galectin network with deviations from the canonical sequence signature. 2. Galectin-Related Protein (GRP). Trends Glycosci. Glycotechnol. 30, SE11-SE20. https://doi.org/10.4052/tigg.1727.1SE.
Mayo, K.H., 2023. Heterologous interactions with galectins and chemokines and their functional consequences. Int. J. Mol. Sci. 24, 14083. https://doi.org/10.3390/ijms241814083.
Mencia, N., Selga, E., Noé, V., Ciudad, C.J., 2011. Underexpression of miR-224 in methotrexate resistant human colon cancer cells. Biochem. Pharmacol. 82, 1572–1582. https://doi.org/10.1016/j.bcp.2011.08.009.
Miranda, A.L., Racca, A.C., Kourdova, L.T., Rojas, M.L., Cruz Del Puerto, M., Rodriguez-Lombardi, G., Salas, A.V., Travella, C., da Silva, E.C.O., de Souza, S.T., Fonseca, E.J. S., Marques, A.L.X., Borbely, A.U., Genti-Raimondi, S., Panzetta-Dutari, G.M., 2022. Krüppel-like factor 6 (KLF6) requires its amino terminal domain to promote villous trophoblast cell fusion. Placenta 117, 139–149. https://doi.org/10.1016/j.placenta.2021.12.006.
Moore, D.L., Blackmore, M.G., Hu, Y., Kaestner, K.H., Bixby, J.L., Lemmon, V.P., Goldberg, J.L., 2009. KLF family members regulate intrinsic axon regeneration ability. Science 326, 298–301. https://doi.org/10.1126/science.1175737.
Pfaffl, M.W., 2001. A new mathematical model for relative quantification in real-time RT-PCR. Nucleic Acids Res. 29, e45.
Plachý, J., 2000. The chicken–a laboratory animal of the class Aves. Folia Biol. (Praha) 46, 17–23.
Pollak, N.M., Hoffman, M., Goldberg, I.J., Drosatos, K., 2018. Krüppel-like factors: Crippling and un-crippling metabolic pathways. JACC Basic Transl Sci 3, 132–156. https://doi.org/10.1016/j.jacbts.2017.09.001.
Ravenhill, B.J., Boyle, K.B., von Muhlinen, N., Ellison, C.J., Masson, G.R., Otten, E.G., Foeglein, A., Williams, R., Randow, F., 2019. The cargo receptor NDP52 initiates selective autophagy by recruiting the ULK complex to cytosol-invading bacteria. Mol. Cell 74 (320–329), e6.
Rodrigues, J.G., Balmaña, M., Macedo, J.A., Poças, J., Fernandes, A., de-Freitas-Junior, J. C.M., Pinho, S.S., Gomes, J., Magalhães, A., Gomes, C., Mereiter, S. and Reis, C.A., 2018. Glycosylation in cancer: Selected roles in tumour progression, immune modulation and metastasis. Cell Immunol 333, 46-57. doi: 10.1016/j.cellimm.2018.03.007.
Sanjurjo, L., Broekhuizen, E.C., Koenen, R.R., Thijssen, V., 2022. Galectokines: The promiscuous relationship between galectins and cytokines. Biomolecules 12, 1286. https://doi.org/10.3390/biom12091286.
Shen, W., Yuan, L., Hao, B., Xiang, J., Cheng, F., Wu, Z., Li, X., 2024. KLF3 promotes colorectal cancer growth by activating WNT1. Aging (Albany NY) 16, 2475–2493. https://doi.org/10.18632/aging.205494.
Su, J., 2018. A brief history of Charcot-Leyden Crystal Protein/galectin-10 research. Molecules 23, 2931. https://doi.org/10.3390/molecules23112931.
Su, J., Cui, L., Si, Y., Song, C., Li, Y., Yang, T., Wang, H., Mayo, K.H., Tai, G., Zhou, Y., 2018. Resetting the ligand binding site of placental protein 13/galectin-13 recovers its ability to bind lactose. Biosci. Rep. 38. https://doi.org/10.1042/BSR20181787.
Sun, Y., Jin, Z., Zhang, X., Cui, T., Zhang, W., Shao, S., Li, H., Wang, N., 2020. GATA binding protein 3 is a direct target of Krüppel-like transcription factor 7 and inhibits chicken adipogenesis. Front. Physiol. 11, 610. https://doi.org/10.3389/fphys.2020.00610.
Swaminathan, G.J., Leonidas, D.D., Savage, M.P., Ackerman, S.J., Acharya, K.R., 1999. Selective recognition of mannose by the human eosinophil Charcot-Leyden crystal protein (galectin-10): a crystallographic study at 1.8 A resolution. Biochemistry 38, 13837–13843. https://doi.org/10.1021/bi990756e.
Troncoso, M.F., Elola, M.T., Blidner, A.G., Sarrias, L., Espelt, M.V., Rabinovich, G.A., 2023. The universe of galectin-binding partners and their functions in health and disease. J. Biol. Chem. 299, 105400. https://doi.org/10.1016/j.jbc.2023.105400.
Turner, J., Crossley, M., 1998. Cloning and characterization of mCtBP2, a co-repressor that associates with basic Krüppel-like factor and other mammalian transcriptional regulators. EMBO J. 17, 5129–5140. https://doi.org/10.1093/emboj/17.17.5129.
Veldman, M.B., Bemben, M.A., Thompson, R.C., Goldman, D., 2007. Gene expression analysis of zebrafish retinal ganglion cells during optic nerve regeneration identifies KLF6a and KLF7a as important regulators of axon regeneration. Dev. Biol. 312, 596–612. https://doi.org/10.1016/j.ydbio.2007.09.019.
Vu, T.T., Gatto, D., Turner, V., Funnell, A.P., Mak, K.S., Norton, L.J., Kaplan, W., Cowley, M.J., Agenes, F., Kirberg, J., Brink, R., Pearson, R.C., Crossley, M., 2011. Impaired B cell development in the absence of Krüppel-like factor 3. J. Immunol. 187, 5032–5042. https://doi.org/10.4049/jimmunol.1101450.
Wälti, M.A., Thore, S., Aebi, M., Künzler, M., 2008. Crystal structure of the putative carbohydrate recognition domain of human galectin-related protein. Proteins 72, 804–808. https://doi.org/10.1002/prot.22078.
Wang, Y., Li, W.Y., Jia, H., Zhai, F.G., Qu, W.R., Cheng, Y.X., Liu, Y.C., Deng, L.X., Guo, S. F., Jin, Z.S., 2017. KLF7-transfected Schwann cell graft transplantation promotes sciatic nerve regeneration. Neuroscience 340, 319–332. https://doi.org/10.1016/j.neuroscience.2016.10.069.
Wang, W., Malcolm, B.A., 1999. Two-stage PCR protocol allowing introduction of multiple mutations, deletions and insertions using QuikChange Site-Directed Mutagenesis. Biotechniques 26, 680–682. https://doi.org/10.2144/99264st03.
Xu, J., Pratt, H.E., Moore, J.E., Gerstein, M.B., Weng, Z., 2022. Building integrative functional maps of gene regulation. Hum. Mol. Genet. 31, R114–R122. https://doi.org/10.1093/hmg/ddac195.
Yuce, K., Ozkan, A.I., 2024. The krüppel-like factor (KLF) family, diseases, and physiological events. Gene 895, 148027. https://doi.org/10.1016/j.gene.2023.148027.
Zhang, J., Yang, C., Brey, C., Rodriguez, M., Oksov, Y., Gaugler, R., Dickstein, E., Huang, C.H., Hashmi, S., 2009. Mutation in *Caenorhabditis elegans* Krüppel-like factor, KLF-3 results in fat accumulation and alters fatty acid composition. Exp. Cell Res. 315, 2568–2580. https://doi.org/10.1016/j.yexcr.2009.04.025.
Zhang, J., Jia, J., Zhao, L., Li, X., Xie, Q., Chen, X., Wang, J., Lu, F., 2016. Down-regulation of microRNA-9 leads to activation of IL-6/Jak/STAT3 pathway through directly targeting IL-6 in HeLa cell. Mol. Carcinog. 55, 732–742. https://doi.org/10.1002/mc.22317.
Zhang, Q.H., Ye, M., Wu, X.Y., Ren, S.X., Zhao, M., Zhao, C.J., Fu, G., Shen, Y., Fan, H.Y., Lu, G., Zhong, M., Xu, X.R., Han, Z.G., Zhang, J.W., Tao, J., Huang, Q.H., Zhou, J., Hu, G.X., Gu, J., Chen, S.J., Chen, Z., 2000. Cloning and functional analysis of cDNAs with open reading frames for 300 previously undefined genes expressed in CD34+ hematopoietic stem/progenitor cells. Genome Res. 10, 1546–1560. https://doi.org/10.1101/gr.140200.
Zhao, L., Zhang, Y., Liu, J., Yin, W., Jin, D., Wang, D., Zhang, W., 2019. miR-185 Inhibits the proliferation and invasion of non-small cell lung cancer by targeting KLF7. Oncol. Res. 27, 1015–1023. https://doi.org/10.3727/096504018X15247341491655.
Zheng, J., Zhang, M., Zhang, L., Ding, X., Li, W., Lu, S., 2018. HSPC159 promotes proliferation and metastasis by inducing epithelial-mesenchymal transition and activating the PI3K/Akt pathway in breast cancer. Cancer Sci. 109, 2153–2163. https://doi.org/10.1111/cas.13631.
Zheng, Y., Zhang, H., Xiao, C., Deng, Z., Fan, T., Zheng, B., Li, C., He, J., 2023. KLF12 overcomes anti-PD-1 resistance by reducing galectin-1 in cancer cells. J. Immunother. Cancer 11, e007286.
Zhou, D., Sun, J., Zhao, W., Zhang, X., Shi, Y., Teng, M., Niu, L., Dong, Y., Liu, P., 2006. Expression, purification, crystallization and preliminary X-ray characterization of the GRP carbohydrate-recognition domain from Homo sapiens. Acta Crystallogr. Sect. F Struct. Biol. Cryst. Commun. 62, 474–476. https://doi.org/10.1107/S1744309106012875.
Zhou, D., Ge, H., Sun, J., Gao, Y., Teng, M., Niu, L., 2008. Crystal structure of the C-terminal conserved domain of human GRP, a galectin-related protein, reveals a function mode different from those of galectins. Proteins 71, 1582–1588. https://doi.org/10.1002/prot.22003.